Rail Roughness Identification Via On-Board Acceleration Data and Bayesian Filtering

CHARIKLEIA D. STOURA, VASILIS K. DERTIMANIS and ELENI N. CHATZI

ABSTRACT

The global demand for transportation has resulted in extensive expansion of railway networks. However, ensuring the safety, reliability, and efficiency of these rapidly expanding railway infrastructures requires monitoring of their structural health. Focusing on tracks, traditional visual inspections and portable measuring devices are commonly used to gather geometric data for diagnosing and predicting track defects. In recent years, railway operators worldwide have employed specialized diagnostic vehicles equipped with optical and inertial sensors to collect track data and assess its condition. This approach has revolutionized rail condition assessment by introducing a mobile data acquisition platform for track inspection. Nevertheless, deploying these specialized vehicles disrupts regular rail service, limiting their frequency of operation and the continuous collection of rail data. To address this limitation, this study explores an on-board monitoring (OBM) method that focuses on collecting vibration data from traveling trains. The proposed methodology involves gathering acceleration data from axle boxes of trains running at normal speeds. What sets this approach apart is its use of realistic train models and the consideration of the dynamic interaction between the trains and tracks, which is typically oversimplified. The train model employed is simplified to reduce computational requirements. The identification process relies on sequential Bayesian inference for joint input and state estimation. By estimating the input, the relevant rail roughness profile can be identified, thereby providing information on the presence of isolated defects, such as welded joints and squats, along the track system.

INTRODUCTION

Systematic monitoring and regular maintenance of railway infrastructures are crucial to ensure the safety of rail transport. Although reliable, traditional methods relying on visual inspections and on-site measurements are no longer sufficient to meet the growing demand for monitoring large sections of railways. As a result, roving implementations

Charikleia D. Stoura, Postdoctoral Fellow, Email: charikleia.stoura@ibk.baug.ethz.ch. Institute of Structural Engineering, Department of Civil, Environmental and Geomatic Engineering, ETH Zurich, Zurich, 8093, Switzerland.

using Track Recording Vehicles have gained popularity in recent years [1]. These vehicles are equipped with optical (such as laser scanners and high-speed cameras) and inertial sensors (including gyroscopes and inclinometers) to collect geometric data from the rails. This data provides insights into specific irregularities on the tracks, enabling accurate identification of isolated defects. However, these vehicles can only operate when regular rail service is suspended, limiting their ability to provide continuous information about the track's condition [2].

An alternative approach involves using in-service trains equipped with low-cost monitoring systems, such as accelerometers. These accelerometers can be mounted on various train components, including axle boxes, bogies, and car bodies, allowing for a continuous supply of vibration data. Railway operators are increasingly improving the monitoring systems on in-service trains primarily for vehicle condition monitoring, but these systems can also facilitate monitoring of the rail infrastructure, including tracks and rail bridges. For example, the ICN train of the Swiss Federal Railways (SBB) is equipped with accelerometers in different locations [3]. This abundance of acceleration monitoring data requires appropriate processing techniques.

One approach to handle such data involves using signal decomposition techniques like wavelet transform [4] or mixed filtering approaches such as Kalman, band-pass, and compensation filters [5]. These methods focus solely on processing the acquired data without considering the dynamic interaction between trains and tracks. However, a recent study by Dertimanis et al. [2] incorporated the dynamic train-track interaction into the identification of rail defects using acceleration data collected from axle boxes of a simple train model. This study showed promising results in identifying rail roughness profiles from in-service trains.

Motivated by the need to develop comprehensive methods to efficiently monitor the conditions of tracks, this work proposes an indirect approach to identify rail roughness profiles using data collected from realistic traversing trains. The proposed method takes into account the physics of the dynamic train-track interaction phenomenon [6] and combines substructure-based dynamics [7] with Bayesian inference methods to perform rail roughness identification [8]. The key component is the employment of a real three-dimensional (3D) train model of SBB operating on tracks with rail roughness also measured by SBB, ensuring a realistic scenario setting.

REDUCED TRAIN-TRACK SYSTEM FOR RAIL ROUGHNESS IDENTIFICATION

The train is modeled via rigid bodies connected with springs and dampers, which constitute the vehicle's suspension system. The track system is modeled via rigid beams with a rough surface on which the train runs. The equation of motion (EOM) of the train can be written as:

$$\mathbf{m}^{\mathrm{v}}\ddot{\mathbf{u}}^{\mathrm{v}}(t) + \mathbf{c}^{\mathrm{v}}\dot{\mathbf{u}}^{\mathrm{v}}(t) + \mathbf{k}^{\mathrm{v}}\mathbf{u}^{\mathrm{v}}(t) = \mathbf{W}^{\mathrm{v}}\boldsymbol{\lambda}(t) \tag{1}$$

where $\mathbf{u}^{\mathrm{v}}(t)$ is the response vector of the train, and $\dot{\square}$ indicates differentiation with respect to time t. The $\mathbf{u}^{\mathrm{v}}(t)$ vector contains translational and rotational degrees of freedom (DOFs). $\mathbf{m}^{\mathrm{v}}$ is the mass matrix of the train, and $\mathbf{c}^{\mathrm{v}}$ and $\mathbf{k}^{\mathrm{v}}$ are, respectively, the damping and stiffness matrices that emanate from the train's suspension system. $\boldsymbol{\lambda}(t)$ is the

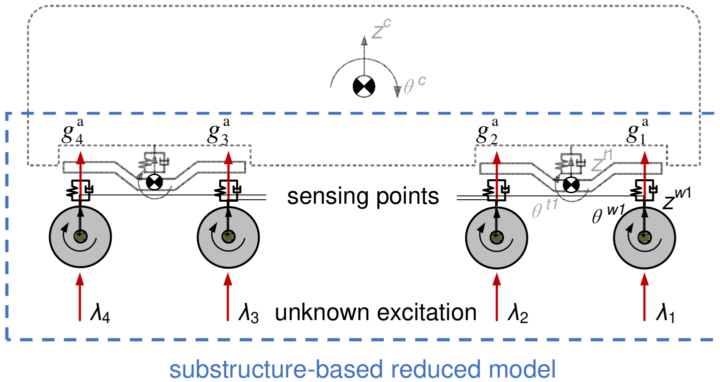

Figure 1. Schematic representation of the full train mode and the reduced, substructure-based model for joint input-state estimation.

contact force vector between the train and the underlying track system, and $\mathbf{W}^{\mathrm{v}}$ is the contact direction matrix connecting the DOFs of the train to the contact force elements. The elastic normal contact force [9] can be written as:

$$\boldsymbol{\lambda}(t) = k^{\mathrm{H}}\mathbf{r}_{\mathrm{c}}(x) \tag{2}$$

where k^{H} is the contact stiffness between the train wheels and the rail, and $\mathbf{r}_{\mathrm{c}}(x)$ is the rail roughness vector of the roughness profile at each contact point between the rails and the wheels. The EOM of the train (Eq. (1)) can be written in state-space space form as:

$$\dot{\mathbf{x}}(t) = \mathbf{A}_{\mathrm{c}}\mathbf{x}(t) + \mathbf{B}_{\mathrm{c}}\boldsymbol{\lambda}(t) \tag{3}$$

where $\dot{\mathbf{x}}\,(t)$ is the state vector:

$$\mathbf{x}(t) = \begin{bmatrix} \mathbf{u}^{\mathrm{v}}(t) \\ \dot{\mathbf{u}}^{\mathrm{v}}(t) \end{bmatrix} \tag{4}$$

$\boldsymbol{\lambda}(t)$ is the input vector, and $\mathbf{A}_{\mathrm{c}}$ and $\mathbf{B}_{\mathrm{c}}$ are, respectively, the system and input matrices of the system:

$$\mathbf{A}_{\mathrm{c}} = \begin{bmatrix} \mathbf{0} & \mathbf{I} \\ -\left(\mathbf{m}^{\mathrm{v}}\right)^{-1}\mathbf{k}^{\mathrm{v}} & -\left(\mathbf{m}^{\mathrm{v}}\right)^{-1}\mathbf{c}^{\mathrm{v}} \end{bmatrix}, \quad \mathbf{B}_{c} = \begin{bmatrix} \mathbf{0} \\ -\left(\mathbf{m}^{\mathrm{v}}\right)^{-1}\mathbf{W}^{\mathrm{v}} \end{bmatrix}. \tag{5}$$

Assuming that acceleration measurement data are available, the output vector can be written as:

$$\mathbf{y}\,(t) = \mathbf{C}_{\mathrm{c}}\mathbf{x}\,(t) + \mathbf{D}_{\mathrm{c}}\boldsymbol{\lambda}\,(t) \tag{6}$$

where the output matrix $\mathbf{C}_{\mathrm{c}}$ and feedforward matrix $\mathbf{D}_{\mathrm{c}}$ are:

$$\mathbf{C}_{\mathrm{c}} = \begin{bmatrix} -\mathbf{W}^{\mathrm{a}}(\mathbf{m}^{\mathrm{v}})^{-1}\mathbf{k}^{\mathrm{v}} & -\mathbf{W}^{\mathrm{a}}(\mathbf{m}^{\mathrm{v}})^{-1}\mathbf{c}^{\mathrm{v}} \end{bmatrix}, \quad \mathbf{D}_{\mathrm{c}} = \mathbf{W}^{\mathrm{a}}(\mathbf{m}^{\mathrm{v}})^{-1}\mathbf{W}^{\mathrm{v}} \tag{7}$$

with $\mathbf{W}^{\mathrm{a}}$ being the selection matrix of accelerations connecting the output data with the DOFs of the train.

To reduce the computational cost involved in the identification task, the train model is reduced via the adoption of a substructure-based reduction scheme. Model reduction, based on substructuring, allows for monitoring only a part of the structure [7]. The substructure to be monitored depends on the location of the input and the installed sensors, where the output is measured. For example, in the case of roughness identification via measurements from the axle boxes, the monitored components can be the respective wheelsets (where the input is applied) and axle boxes (where the measurements are collected from). To this end, the train model is partitioned into the vehicle's upper substructure, consisting of the car body and bogies, and the vehicle's lower substructure, consisting of the wheelsets and axle boxes. Subsequently, Eq. (1) can be written in a partitioned form as:

$$\begin{bmatrix} \mathbf{m}^{\mathrm{u}} & \mathbf{0} \\ \mathbf{0} & \mathbf{m}^{\mathrm{l}} \end{bmatrix} \begin{bmatrix} \ddot{\mathbf{u}}^{\mathrm{u}}(t) \\ \ddot{\mathbf{u}}^{\mathrm{l}}(t) \end{bmatrix} + \begin{bmatrix} \mathbf{c}^{\mathrm{u}} & \mathbf{c}^{\mathrm{ul}} \\ \mathbf{c}^{\mathrm{lu}} & \mathbf{c}^{\mathrm{l}} \end{bmatrix} \begin{bmatrix} \dot{\mathbf{u}}^{\mathrm{u}}(t) \\ \dot{\mathbf{u}}^{\mathrm{l}}(t) \end{bmatrix} + \begin{bmatrix} \mathbf{k}^{\mathrm{u}} & \mathbf{k}^{\mathrm{ul}} \\ \mathbf{k}^{\mathrm{lu}} & \mathbf{k}^{\mathrm{l}} \end{bmatrix} \begin{bmatrix} \mathbf{u}^{\mathrm{u}}(t) \\ \mathbf{u}^{\mathrm{l}}(t) \end{bmatrix} = \begin{bmatrix} \mathbf{0} \\ \mathbf{W}^{\mathrm{l}} \end{bmatrix} \boldsymbol{\lambda}(t) \tag{8}$$

where superscript $\square^{\mathrm{u}}$ denotes the train vehicle's upper part and $\square^{\mathrm{l}}$ the lower part. Following, the substructure of interest, i.e., the lower part, is isolated as:

$$\mathbf{m}^{\mathrm{l}}\ddot{\mathbf{u}}^{\mathrm{l}}(t) + \mathbf{c}^{\mathrm{l}}\dot{\mathbf{u}}^{\mathrm{l}}(t) + \mathbf{k}^{\mathrm{l}}\mathbf{u}^{\mathrm{l}}(t) = \mathbf{W}^{\mathrm{l}}\boldsymbol{\lambda}(t) - \mathbf{c}^{\mathrm{lu}}\dot{\mathbf{u}}^{\mathrm{u}}(t) - \mathbf{k}^{\mathrm{lu}}\mathbf{u}^{\mathrm{u}}(t) \tag{9}$$

and can be written as:

$$\mathbf{m}^{\mathrm{l}}\ddot{\mathbf{u}}^{\mathrm{l}}(t) + \mathbf{c}^{\mathrm{l}}\dot{\mathbf{u}}^{\mathrm{l}}(t) + \mathbf{k}^{\mathrm{l}}\mathbf{u}^{\mathrm{l}}(t) = \mathbf{W}^{\mathrm{l}}\boldsymbol{\lambda}(t) + \mathbf{g}(t) \tag{10}$$

where $\mathbf{W}^{\mathrm{l}}\boldsymbol{\lambda}(t)$ are the external forces and $\mathbf{g}(t)$ are the internal forces acting on the substructure. Eq. (10) can then be expanded as:

$$\begin{bmatrix} \mathbf{m}^{\mathrm{w}} & \mathbf{0} \\ \mathbf{0} & \mathbf{m}^{\mathrm{a}} \end{bmatrix} \begin{bmatrix} \ddot{\mathbf{u}}^{\mathrm{w}}(t) \\ \ddot{\mathbf{u}}^{\mathrm{a}}(t) \end{bmatrix} + \begin{bmatrix} \mathbf{c}^{\mathrm{w}} & \mathbf{c}^{\mathrm{wa}} \\ \mathbf{c}^{\mathrm{aw}} & \mathbf{c}^{\mathrm{a}} \end{bmatrix} \begin{bmatrix} \dot{\mathbf{u}}^{\mathrm{w}}(t) \\ \dot{\mathbf{u}}^{\mathrm{a}}(t) \end{bmatrix} + \begin{bmatrix} \mathbf{k}^{\mathrm{w}} & \mathbf{k}^{\mathrm{wa}} \\ \mathbf{k}^{\mathrm{aw}} & \mathbf{k}^{\mathrm{a}} \end{bmatrix} \begin{bmatrix} \mathbf{u}^{\mathrm{w}}(t) \\ \mathbf{u}^{\mathrm{a}}(t) \end{bmatrix} = \begin{bmatrix} \mathbf{W}^{\mathrm{w}}\boldsymbol{\lambda} \\ \mathbf{0} \end{bmatrix} + \begin{bmatrix} \mathbf{0} \\ \mathbf{g}^{\mathrm{a}} \end{bmatrix} \tag{11}$$

where superscript $\square^{\mathrm{w}}$ denotes the wheelset substructure and $\square^{\mathrm{a}}$ indicates the axle boxes substructure, connecting the lower part of the train to the upper part. Consequently, the contact force vector $\boldsymbol{\lambda}$ acts only on the wheelsets and encompasses the external forces applied at the contact point. At the same time, $\mathbf{g}^{\mathrm{a}}$ is an internal force vector acting on the axle boxes and is typically orders of magnitude smaller than the contact force vector [10]. Thus, ignoring $\mathbf{g}^{\mathrm{a}}$ as small, Eq. (10) can be written in state-space form, similarly to Eq. (3).

The identification of rail roughness relies on a Bayesian inference approach. To apply such an approach, the state space system needs first to be discretized in time. For the discretization of the state-space system, a sampling rate f_{s} is adopted, corresponding to a discretization time interval $t = kT_{\mathrm{s}}$. The discretization of the pertinent state-space matrices follows a bilinear transform, also known as the Tustin method. The Tustin method performs integration based on a trapezoidal rule and yields the best frequency-domain match between the continuous and discretized systems [11]. This assumption emerges from our effort to accurately reconstruct the input vector, which herein comprises the roughness profile (i.e., a random time-series), as indicated by Eq. (2), in a reliable and efficient manner. Accordingly, the identification of the roughness profile of the rails relies on a recursive Bayesian inference approach that allows for concurrent identification of the states and inputs to the reduced-order train system via a Dual Kalman Filter (DKF), described in detail in the study of Eftekhar Azam et al. [8].

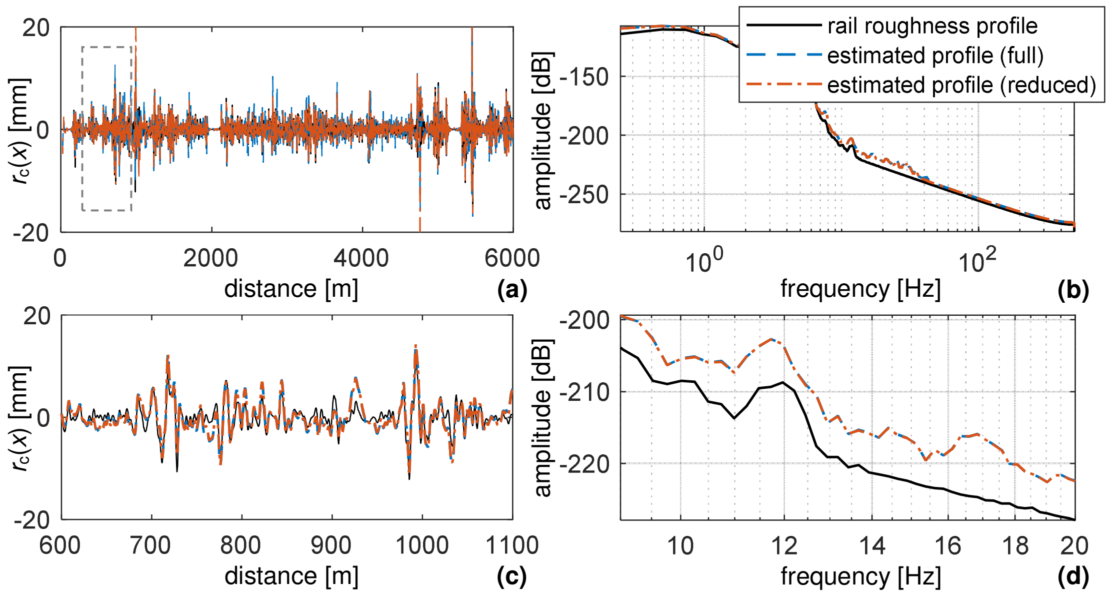

Figure 2. (a) Response history and (b) one-sided Power Spectral Density of the true (blue) and estimated via DKF rail roughness profile with the full train model (green) and the reduced substructure-based train model (orange), (c) zoom-in of (a) between 600 m and 1100 m, and (d) zoom-in of be between 9 Hz and 20 Hz

ON-BOARD MEASUREMENT DATA FROM AN SBB DIAGNOSTIC VEHICLE RUNNING ON THE SBB NETWORK

This section employs a realistic train model of the SBB network running on a roughness profile on rigid ground, also measured by SBB [12]. Both train and track systems are modeled via the SIMPACK software [13]. The train represents the diagnostic (gDfZ) vehicle of SBB [14]. This train-track model simulated in SIMPACK software is used to produce measurement data of the axle boxes at a sampling frequency $f_s = 1000$ Hz. The acceleration data is then used in the identification task.

The identification task, i.e., the inverse modeling of the system, is realized in MATLAB software [15]. The total number of states is 144 of the vehicle, and the number of inputs is eight, corresponding to the eight wheels of the four wheelsets of the vehicle. The number of outputs is four, corresponding to the four accelerometers mounted on the diagnostic vehicle. To reduce the computational effort of the identification task, we employ the substructure-based approach of the previous section. In this case, the wheelset-axle box system is separated from the upper part of the train (car body and bogies), and internal forces arise at the connection with the upper part, as in Eq. (11). Figure 1 illustrates the retained bodies. The total number of states retained is 64.

The estimation of roughness profiles follows the DKF with a bilinear transformation assumed for the discretization of the state-space system. The covariance matrix of the process noise is set to $\mathbf{Q}_w = 10^{-10} \cdot \mathbf{I}_1$, the measurement noise covariance matrix is $\mathbf{Q}_r = 10^{-1} \cdot \mathbf{I}_2$, and the covariance matrix of the input noise is estimated as $\mathbf{Q}_v = 10^{-5} \cdot \mathbf{I}_3$, based on an L-curve analysis. Figure 2 plots the response history (Figure 2(a) and (c)) and one-sided Power Spectral Density (PSD) (Figure 2(b) and (d)) of the estimated profile of the rails when using the reduced-order model and the full train model. For comparison, Figure 2 also shows the response history and PSD of the roughness profile used in the forward analysis to generate measurement data, which is referred to as the *true roughness profile*. The identified profile shows very good agreement with the true roughness profile in both space (Figure 2(a) and (c)) and temporal frequency domains (Figure 2(b) and (d)). Lastly, the identified roughness profile according to the substructure-based reduced train model is in excellent agreement with that exported based on the full train model, as shown in Figure 2.

Finally, the computational effort for the reduced-order train model is significantly lower than that of the full-order train model (4.7 times faster), demonstrating the importance of reduced-order models in inverse problems, especially when online schemes are of interest.

CONCLUDING REMARKS

This study presents an indirect approach for estimating rail roughness profiles using on-board monitoring data from in-service trains. The proposed methodology takes into account the dynamic interaction between trains and tracks and proposes a model-based Bayesian inference method for roughness identification. A joint input-state estimation scheme is employed to estimate the system input and state. To reduce the computational effort involved, the vehicle model is simplified using a substructure-based scheme.

The efficacy of the proposed methodology is evaluated through a case study. This case study utilizes data from a real diagnostic vehicle of SBB running on the SBB rail network. The substructure-based reduced model yields accurate results when compared to the roughness profile used for the generation of the measured acceleration data. At the same time, compared to the full train model, it leads to improved computational efficiency, which could be of particular interest in the case of near real-time identification applications.

The proposed methodology has been applied to a diagnostic vehicle of SBB, aiming to develop a comprehensive approach applicable to in-service trains. While the focus has been on longitudinal roughness profiles in the vertical direction, the approach can be extended to the lateral direction as well. The ultimate goal is to enable continuous monitoring of track conditions for timely fault identification and maintenance.

ACKNOWLEDGMENT

This study is supported by the Stavros Niarchos Foundation through the ETH Zürich Foundation and the ETH Zürich Postdoctoral Fellowship scheme. The authors would like to thank Claudia Kossmann from SBB for her input and constructive comments.

REFERENCES

1. Weston, P., C. Roberts, G. Yeo, and E. Stewart. 2015. “Perspectives on railway track geometry condition monitoring from in-service railway vehicles,” *Vehicle System Dynamics*, 53:1063–1091, doi:10.1080/00423114.2015.1034730.

2. Dertimanis, V., M. Zimmermann, F. Corman, and E. Chatzi. 2019. "On-Board Monitoring of Rail Roughness via Axle Box Accelerations of Revenue Trains with Uncertain Dynamics," in *Model Validation and Uncertainty Quantification, Volume 3. Conference Proceedings of the Society for Experimental Mechanics Series*, pp. 167–171.
3. Hoelzl, C., V. Dertimanis, M. Landgraf, L. Ancu, M. Zurkirchen, and E. Chatzi. 2022. "On-board monitoring for smart assessment of railway infrastructure: A systematic review," in *The Rise of Smart Cities*, Advanced Structural Sensing and Monitoring Systems, pp. 223–259.
4. Bocciolone, M., A. Caprioli, A. Cigada, and A. Collina. 2007. "A measurement system for quick rail inspection and effective track maintenance strategy," *Mechanical Systems and Signal Processing*, 3:1242–1254, doi:10.1016/j.ymssp.2006.02.007.
5. Lee, J., S. Choi, S. Kim, C. Park, and Y. Kim. 2012. "A mixed filtering approach for track condition monitoring using accelerometers on the axle box and bogie," *IEEE Transactions on Instrumentation and Measurement*, 61:749–758, doi:10.1109/TIM.2011.2170377.
6. Stoura, C. and E. Dimitrakopoulos. 2020. "Additional damping effect on bridges because of vehicle-bridge interaction," *Journal of Sound and Vibration*, 476:115294, doi:10.1016/j.jsv.2020.115294.
7. Tatsis, K., V. Dertimanis, C. Papadimitriou, E. Lourens, and E. Chatzi. 2021. "A general substructure-based framework for input-state estimation using limited output-only measurements," *Mechanical Systems and Signal Processing*, 150:107223.
8. Azam, S. E., E. Chatzi, and C. Papadimitriou. 2015. "A dual Kalman filter approach for state estimation via output-only acceleration measurements," *Mechanical Systems and Signal Processing*, 60–61:866–886, doi:10.1016/j.ymssp.2015.02.001.
9. Johnson, K. 1987. *Contact Mechanics*, Cambridge University Press, Cambridge, United Kingdom.
10. Stoura, C. and E. Dimitrakopoulos. 2020. "A Modified Bridge System method to characterize and decouple vehicle-bridge interaction," *Acta Mech.*, 231:3825–3845.
11. Franklin, G., J. Powell, and M. Workman. 1998. *Digital Control of Dynamic Systems*, Addison-Wesley, Menlo Park.
12. Hoelzl, C., L. Keller, T. Simpson, C. Stoura, C. Kossmann, and E. Chatzi. 2023. "Data-Driven Railway Vehicle Parameter Tuning Using Markov-Chain Monte Carlo Bayesian Updating," in *Conference Proceedings of XII Conference on Structural Dynamics (EURODYN 2023)*.
13. Dassault Systémes. 2021, "SIMPACK," `https://www.3ds.com/products-services/simulia/products/simpack/`.
14. Kossman, C. 2021, "SIMPACK gezogenes Diagnosfahrzeug (gDfZ) vehicle model," SBB Infrastructure.
15. MathWorks. 2021, "MATLAB," `https://ch.mathworks.com/de/products/matlab.html`.